tvst

Article

Driving With Hemianopia VII: Predicting Hazard Detection With Gaze and Head Scan Magnitude

Garrett Swan[1], Steven W. Savage[1], Lily Zhang[1], and Alex R. Bowers[1]

[1] Schepens Eye Research Institute of Massachusetts Eye and Ear, Department of Ophthalmology, Harvard Medical School, Boston, MA, USA

Correspondence: Garrett Swan, Schepens Eye Research Institute of Massachusetts Eye and Ear, Department of Ophthalmology, Harvard Medical School, 20 Staniford St., Boston, MA 02114, USA.
e-mail: gsp.swan@gmail.com

Received: July 22, 2020
Accepted: November 26, 2020
Published: XXXXX XX, 2020

Keywords: compensatory gaze scans; hemianopic visual field loss; driving simulation

Citation: Swan G, Savage SW, Zhang L, Bowers AR. Driving with hemianopia VII: Predicting hazard detection with gaze and head scan magnitude. Trans Vis Sci Tech. 2020;0(0):2876, https://doi.org/10.1167/tvst.0.0.2876

Purpose: One rehabilitation strategy taught to individuals with hemianopic field loss (HFL) is to make a large blind side scan to quickly identify hazards. However, it is not clear what the minimum threshold is for how large the scan should be. Using driving simulation, we evaluated thresholds (criteria) for gaze and head scan magnitudes that best predict detection safety.

Methods: Seventeen participants with complete HFL and 15 with normal vision (NV) drove through 4 routes in a virtual city while their eyes and head were tracked. Participants pressed the horn as soon as they detected a motorcycle (10 per drive) that appeared 54 degrees eccentricity on cross-streets and approached toward the driver.

Results: Those with HFL detected fewer motorcycles than those with NV and had worse detection on the blind side than the seeing side. On the blind side, both safe detections and early detections (detections before the hazard entered the intersection) could be predicted with both gaze (safe 18.5 degrees and early 33.8 degrees) and head (safe 19.3 degrees and early 27 degrees) scans. However, on the seeing side, only early detections could be classified with gaze (25.3 degrees) and head (9.0 degrees).

Conclusions: Both head and gaze scan magnitude were significant predictors of detection on the blind side, but less predictive on the seeing side, which was likely driven by the ability to use peripheral vision. Interestingly, head scans were as predictive as gaze scans.

Translational Relevance: The minimum scan magnitude could be a useful criterion for scanning training or for developing assistive technologies to improve scanning.

Introduction

For those with hemianopic field loss (HFL), scanning (looking) toward the side of their visual field loss (i.e. the blind side) is necessary for mitigating the effects of visual field loss in interacting with the environment. Scanning is especially critical in those with HFL who drive, which is permitted in some US states[1] as well as some other countries (e.g. the United Kingdom, Europe, Australia, and Canada).[2–5] In order to detect hazards on their blind side, these individuals need to scan far enough into the blind side (at least as far as the object of interest) to compensate for the lack of peripheral vision on that side. Prior research suggests that people with HFL often fail to scan sufficiently, resulting in impaired detection of blind side objects in virtual driving tasks.[6–11] In real-world driving, failure to scan far enough means that a blind side hazard might not be detected, which could result in a collision. Those with HFL that do scan further into their blind side tend to detect hazards on that side more than those that do not[9] and are more likely to pass driving tests.[10] The current study focused on the minimum scan magnitude needed for detection of peripheral hazards at intersections.

Programs have been implemented aimed at training patients with HFL to compensate for their visual field loss by increasing the frequency and/or magnitude of scans toward their blind side.[12,13] In some programs, training involves teaching patients to make a large scan into the blind side,[14,15] which gives the individual an opportunity to quickly see objects on the blind side that may be task relevant.[16–18] This strategy of making

a large scan into the blind side improved detection of peripheral stimuli in mobility related tasks[12] and visual scanning of some participants with HFL in a practical driving test.[14] An important consideration, however, in designing such a training program is how large this "large" scan needs to be. In a training program aimed at improving scanning while walking, De Haan and colleagues[12] recommended an eye saccade that reaches 44 degrees, which is near the maximum that can be achieved without a head movement.[19] Tant and colleagues[14] similarly recommended a singular large eye saccade in a scanning training program for drivers with hemianopia. Yet, when walking, most individuals rarely make eye saccades over 15 degrees.[20] Therefore, it is not clear whether there is a minimum threshold (i.e. criterion) for the size of the large scan that successfully and meaningfully predicts detection, and whether that minimum threshold may be task dependent. Here, we address these questions within the context of scanning on approach to intersections, where a large field of view (e.g. 180 degrees at a 4-way intersection) needs to be checked for approaching hazards, typically requiring large gaze scans comprising head as well as eye movements.[21,22]

We aim to identify how far an individual with HFL may need to scan into the blind side by evaluating gaze scan magnitude as a predictor of hazard detection at intersections using a binary classification approach. Additionally, we will measure if the head scan component of the gaze scan predicts detection, given that it is easier to track head scan magnitude than gaze scan magnitude and may be a suitable surrogate for gaze.[23,24] Further, we aim to determine if gaze and head scan magnitudes are predictive of detection on the seeing side in those with HFL and in participants with normal vision (NV). Finally, we will examine whether prediction performance changes when we consider if the detection was made with enough time to make a safe driving maneuver, which takes into account the speed of detection and the velocity of the car at the time of detection. If gaze and head scan magnitude does significantly predict detection, then the criterion (i.e. the threshold in eccentricity that best predicts detection from no detection) may be useful in rehabilitation to train individuals to scan at least as far as that criterion.

Methods

Participants

Thirty-two individuals with HFL and 21 age-similar NV controls were recruited to participate in the experiment. All participants had visual acuity better than 20/40. Of those screened for HFL, seven were excluded because they had quadrantanopia rather than complete homonymous hemianopia (Goldman perimeter, V4e target). Those with HFL were screened for spatial neglect but none tested positive (they would have been excluded if they had 2 of the following: exceeded 4 missed bells on one side in Gauthier bells test[25] or exceeded 2 missed lines or deviated by >11% from the middle in Schenkenberg line bisection).[26,27] Fourteen participants (8 with HFL and 6 with NV) experienced simulator sickness in practice drives prior to the experimental drives, and were thus not included in data analyses.

After excluding the above participants, 17 individuals with HFL and 15 age-similar NV controls were included in analyses (Table 1). Although the majority of our participants with HFL developed visual field loss following a stroke (12 of 17), four developed HFL following complications from surgery and one developed HFL following a fall. Only 2 of the participants with HFL were current drivers compared to 14 of the NV participants. One participant with NV had stopped driving but was nevertheless included in analyses as their detection and gaze and head scanning data did not differ in any respect from that of the other participants with NV. Participants with HFL who were former drivers and had stopped driving for a median of 5 years (interquartile range [IQR] = 2.3 to 12.8 years) prior to the study and 13 of 17 had at least 3 years of driving experience prior to the onset of HFL.

Prior to signing informed consent, the nature and possible consequences of the experiment were explained to the participants. The study followed the tenets of the Declaration of Helsinki and was approved by the institutional review board at the Schepens Eye Research Institute.

Materials

Driving Simulator and Eye Tracker

Participants drove in a driving simulator (LE-1500, FAAC Corp., Ann Arbor, MI) that consisted of five 42-inch LCD monitors (LG M4212C-BA, native resolution of 1366 × 768 pixels) with a total 225 degrees horizontal field of view and a 32 degrees vertical field of view on the center screen. The driving simulator included components typically found in an automatic transmission motor vehicle, such as a steering wheel, accelerator and brake pedals, ignition switch, turn signals, seat, and air conditioning. Rear-view and side-view mirrors were inset on the center and left and right monitors, respectively, and a dashboard with

Table 1. Participant Demographic and Visual Characteristics

	HFL, $n = 17$	NV, $n = 15$
Current driver, *n*	2 (12%)	14 (93%)
Male, *n*	15 (88%)	12 (80%)
Race, *n* reported white	16 (94%)	12 (80%)
Age, y, mean (SD)	55.8 (19.8)	54.0 (19.1)
Visual acuity, LogMAR, mean (SD) Snellen equivalent	0.05 (0.20) 20/23	0.00 (0.20) 20/20
MoCA score, mean (SD)	24.4 (5.3)	28.6 (2.1)
Right side HFL, *n*	8 (47%)	NA
Hemianopia caused by stroke, *n*	12 (70.6%)	NA
Years since onset, median (IQR)	4.7 (0.8 to 13)	NA

LogMAR, logarithm of the minimum angle of resolution; MoCA, Montreal Cognitive Assessment.

Figure 1. Image of the driving simulator equipped with six cameras (*red circles*, with the last camera obstructed from view by the chair) located around the driver's seat (2 on the left, 2 on the right, and 2 in the center), which enabled recording of lateral eye and head position up to 90 degrees to the left and right of the driver.

a speedometer and clock were inset on the central monitor. Driving simulator data, which included the position of the vehicle, its speed and heading, and information about other scripted vehicles (i.e. the motorcycle hazards), were collected at 30 Hz.

While driving, the participant's eyes and head position were recorded with a SmartEye 6 remote digital camera system at 60 Hz (SmartEye Pro Version 6.1; Goteborg, Sweden, 2015). The SmartEye system could record gaze and head movements up to 180 degrees horizontally (90 degrees toward the left and right). The cameras were positioned around the driver and can be seen in Figure 1. Gaze tracking was achieved using the pupil center-corneal reflection and by combining an estimate of the direction of a 3D profile of the participant's eyes. Head tracking was achieved by estimating the direction of a 3D head model that the system automatically generates using salient features of the face (e.g. eye corners, corners of the mouth, nostrils, and ears).

Virtual World

Individuals drove through a virtual world that resembled a light industrial city with cross traffic, buildings, and traffic signals. Participants drove two unique routes through the virtual world that were scripted using Scenario Toolbox software (version 3.9.4. 25873; FAAC Incorporated). The routes consisted of 28 and 27 intersections, respectively. Only intersections with motorcycle hazards were included in analyses. The posted speed limit was 30 mph (48.3 km/h) with a 35 mph (56.3 km/h) cap to prevent participants from exceeding that speed. In half of the drives, participants were guided through the simulated world by Global Positioning System (GPS) instructions (e.g. "turn right/left at next intersection"), and in the other half, participants were guided with a lead car.[21]

Motorcycle Hazards

Motorcycle hazards approached along the cross-street from the left or right side at 10 of the intersections along each route (Fig. 2). They appeared equally from the left and right sides in a pseudorandom order. There was at least one intersection without a motorcycle between intersections with motorcycles. When the participant's vehicle was 30 meters from the intersection, the motorcycle was triggered to appear on the cross-street at 60 meters from the intersection (at an eccentricity of about 54 degrees). After appearing, the motorcycle drove toward the path of the driver at 45 mph (72.4 km/h), entering the intersection approximately 3 seconds later. Because the motorcycle was programmed to be a hazard, it entered the intersection

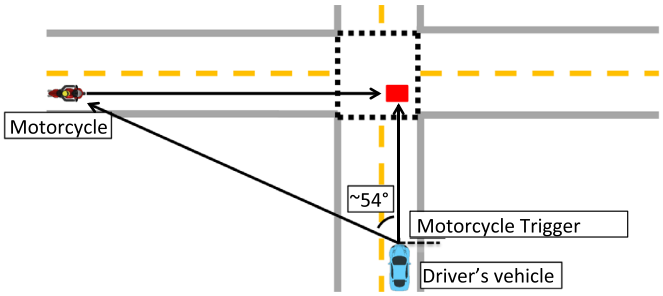

Figure 2. Schematic of a motorcycle hazard at a 4-way intersection showing the motorcycle approaching from the left and with the corresponding collision zone as a red rectangle. Once the driver's vehicle passed the motorcycle trigger (i.e. 30 meters from the white line of the intersection), the motorcycle appeared 60 meters from the white line of the intersection and travelled toward the collision zone at 45 miles per hour (mph; 72.4 km/h).

without slowing down and without obeying any of the usual priority rules. After entering the intersection, the motorcycle continued driving at 45 mph (72.4 km/h) toward the potential collision zone. However, it was programmed to disappear just before entering the collision zone to prevent any psychological stress that may be caused by an actual collision. The parameters were selected empirically based on measurements in a pilot study to create a realistic hazard for a range of participant driving behaviors when approaching an intersection, given that the majority of participants slowed down on approach to the intersection.

Procedure

Prior to the experimental drives, there were two acclimatization drives, which gave the participants an opportunity to practice accelerating and decelerating, stopping at the white line for stop signs and red lights, and taking left and right turns. The acclimatization drives did not have other vehicles or motorcycles. The first drive took place in a rural highway and the second took place in the same virtual city that the participants drove through in the experimental drives. Before proceeding, participants indicated their level of comfort in the simulator and with their control over the motor vehicle, and the experiment continued only if their ratings exceeded our criterion (at least 7 out of 10).

Next, the six cameras of the SmartEye tracking system were calibrated by adjusting their positioning so that they included as much of the participant's face as possible and by adjusting their aperture and focus. Then, a checkerboard pattern was displayed to each camera to inform the system where to expect the participant's head. Participants then completed a practice drive that included all the elements of the experimental drives. They were guided through the city with GPS commands, took left and right turns, and instructed to press the horn as soon as they detected a motorcycle.

After the practice drive, participants' gaze was calibrated using a five-point calibration procedure on the center screen. Participants completed four experimental drives. Each drive scenario typically lasted between 10 and 15 minutes depending on the participants' driving speed. Participants were instructed to drive as they normally would, follow all rules of the road, and to press the horn as soon as they saw a motorcycle. Participants drove through each route twice, once with GPS navigation and once with lead car navigation. The order was counterbalanced, such that the subject did not experience the same route in sequential order. If a participant stepped out of the simulator for a break, re-calibration of the SmartEye tracker was performed prior to continuing.

In the GPS drives, an audio message that contained the navigation instruction was delivered when the participant's vehicle was approximately 70 meters from an intersection. In the Lead Car drives, participants followed the Lead Car (white sedan), which drove at 35 mph (56.3 km/h). The Lead Car made periodic stops to ensure that it stayed within sight of the participant. Participants were instructed to follow the Lead Car at a safe distance.

Participants were not, however, given any specific instructions about how to scan.

Detection Variables

Participants were instructed to press the horn as soon as they saw a motorcycle. Each of these motorcycle events was then classified in the following ways: whether or not there was a detection, whether or not the detection was safe, and whether or not the detection was early (Table 2). Detections only considered whether a horn press occurred following the motorcycle's appearance. Safe and early detections provided more nuanced views of detection, given that detection by itself does not necessarily mean the driver detected with adequate time to make a safe driving maneuver (i.e. safe detection) or detected the hazard before it reached the intersection (i.e. early detection). Early detection was of particular interest, because it was this kind of detection for which a large scan would likely be needed for hazards on the blind side. For events where detection occurred, we calculated reaction time as the difference between when the motorcycle appeared and the time of the horn press. We also recorded the speed of the car at the time of the horn press.

Safe detections were calculated by taking into account the distance and the speed of the driver at

Table 2. Explanations of the Different Classifications of Detection

Detection	Definition Horn Press	Meaning Saw the Motorcycle
Safe	Horn press, PET $>$ 1 s, Deceleration $<$ 4 m/s^2	Saw the motorcycle and responded with enough time to make a safe driving maneuver
Early	Horn press before motorcycle entered intersection	Saw the motorcycle before the motorcycle entered the intersection

PET, post encroachment time.

the time of detection. An individual who is driving slowly may still be driving safely despite being near the collision zone, whereas an individual driving fast may not be safe. In this manner, slow driving may be indicative of a compensatory strategy. To calculate whether a detection was safe or not, we considered two safety metrics, which addressed separate aspects of safety. The first metric was the post-encroachment time (PET[28]), which was defined as the time difference between the two road users entering the collision zone. If the PET was less than 1 second,[28,29] the response was considered unsafe. The second metric was the minimum deceleration rate (in m/s^2) required to stop the participant's car from entering the collision zone before the motorcycle left the collision zone (sometimes referred to as the deceleration to safety time [DST][29]). The required deceleration was calculated using the following equation:

$$\text{Deceleration} = \frac{2\left(S_{jk} - V_{ij}t_{ijk}\right)}{{t_{ijk}}^2}$$

S_{jk} is the distance between the location of the participant's vehicle at the horn press and the location where their vehicle will enter the collision zone; V_{ij} is the velocity of the participant's vehicle at the time of the horn press; and t_{ijk} is the time it would take the participant's vehicle to travel from its location at the time of the horn press to the point at which it enters the collision zone. If the deceleration was greater than 4 m/s^2, the detection was considered unsafe.[28,29] In addition to events where the PET was greater than 1 second or deceleration was greater than 4 m/s^2, events where there was no horn press (motorcycle was not seen) or if the subject's vehicle entered the intersection before the motorcycle were also considered unsafe.

Early detections were calculated by taking into account whether a horn press occurred prior to the motorcycle entering the intersection, given that when the motorcycle entered the intersection, the eccentricity with respect to the driver's path (straight ahead gaze) was approximately 18.5 degrees and would not necessarily require a head movement for the motorcycle to be seen. That is, if the horn press occurred before the motorcycle entered the intersection, the event was considered early, regardless of the speed of the participant's vehicle and/or distance to the intersection. If the horn press occurred after the motorcycle entered the intersection, it was still considered early if the horn press occurred within 0.5 seconds after the motorcycle entered the intersection, given that 0.5 seconds is approximately how long it takes to press the horn following fixation (Savage et al. submitted). Otherwise, the horn press was not considered to be early. Early detections differed from safe detections insomuch that participants would have needed to use peripheral vision or make a scan of at least 18.5 degrees into the direction of the motorcycle to be able to detect it before it reached the intersection. Safe detections, however, could be made by driving slowly enough that the motorcycle could be detected without any scanning or only a small eye scan, given that after the motorcycle entered the intersection it would come very close to the straight-ahead line of sight before disappearing from the scene. In addition, similar to safe detections, events where there was no horn press or if the subject's vehicle entered the intersection before the motorcycle were also considered not early.

Gaze and Head Scanning Magnitude

Visual scanning was quantified in terms of gaze and head scans. Gaze scans were defined as the lateral gaze movements (i.e. toward the left or right) that typically start from near the straight ahead position when scanning on approach to an intersection and end in the periphery up to 90 degrees to the left or 90 degrees to the right. Gaze scans always corresponded to the full extent of the gaze movements, which could be composed of one or more saccades. Typically, individuals return to the straight-ahead position after a gaze scan. These return scans were quantified but not analyzed here because we were only interested in the lateral movements that bring the gaze

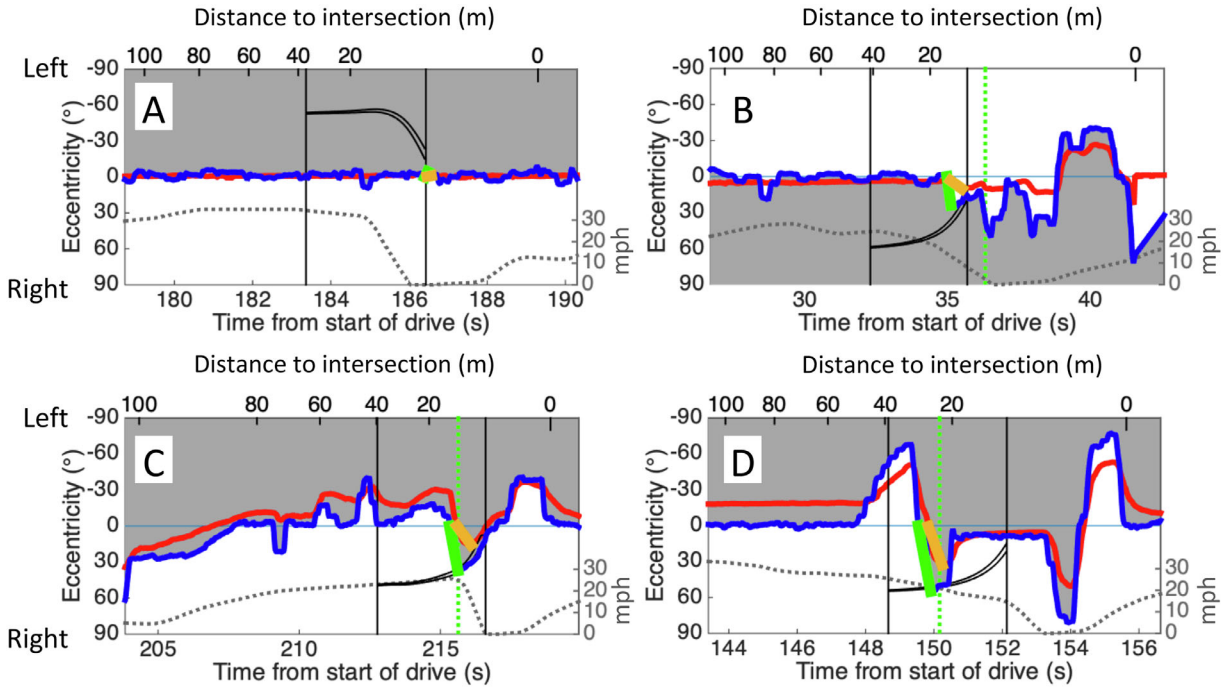

Figure 3. Examples of the gaze (*blue*) and head (*red*) scanning data on approach to intersections (each plot is from one participant). An individual's blind visual field is represented by the shaded area with right hemianopia for the individual in (**B**) and left hemianopia in the others. Here, the *vertical black lines* represent when the motorcycle hazard appeared and disappeared, with the *curved black lines* corresponding to the eccentricity of the motorcycle as it approaches the intersection. The *solid green* and *orange lines* correspond to the maximum gaze scan and corresponding head scan, respectively, while the motorcycle was present. The *vertical dotted green lines* correspond to the time of the horn press (indicating whether the motorcycle was detected). Depending on the speed of the car (*dotted gray line* at the bottom of the figures) at the time of detection or the eccentricity of the motorcycle, the detection could also be safe or early, respectively. In (**A**), there was no horn press, so the event was classified as no detection and also not safe and not early. In (**B**), the horn press was after the motorcycle reached the intersection so the detection was not early, but considered safe given the slow speed of the car. In (**C**), the horn press was before the motorcycle entered the intersection so the detection was early, but considered unsafe given the speed of the car and distance to the intersection at the time of the horn press. In (**D**), the detection was safe and early.

toward the hazard (i.e. away from the straight-ahead position).

Gaze scans were marked automatically using an algorithm called the gaze scan algorithm.[22] In short, the gaze scan algorithm first marks gaze saccades (above 30 degrees per second, longer than 33 ms, and >1 degree in total magnitude), then merges gaze saccades that are headed in the same direction and on the same side of the screen within 400 ms that increase in eccentricity. All gaze scans have a start and end time and eccentricity. Here, the eccentricity at the end of the gaze was used to determine how far an individual scanned (Fig. 3). For each event, we only evaluated the single maximum gaze scan in the direction of the side of the hazard prior to the horn press. If there was a fixation on the motorcycle or an overshoot (i.e. the gaze scan went beyond the motorcycle) followed by a horn press, then the gaze scan that brought the gaze to or passed the motorcycle was used. If there was no fixation on the motorcycle and the motorcycle was still detected (i.e. motorcycle was detected using peripheral vision), then the furthest gaze scan prior to the horn press was used. If the motorcycle was not detected, then the furthest gaze scan prior to the motorcycle disappearing was used. If there was no gaze scan while the motorcycle was on the screen, then that event was coded as having a gaze scan equal to the furthest gaze eccentricity, which was often near 0 degrees.

In addition to tracking gaze movements, head movements were also recorded, given that gaze scans could be made independent of head movements. Head scans were defined as the local minimum and maximum of the head eccentricity with respect to a gaze scan. That is, every gaze scan had a corresponding head scan. Head scans without a corresponding gaze scan were rare and would not be related to hazard detection. In gaze scans without a head movement component (i.e. an eye-only scan), the head scan was marked at the furthest head eccentricity, which could be near or less than 0 degrees.

For both gaze and head scans, we have collapsed across the left/right sides, such that the eccentricity described below refers to a scan away from the intersection toward the side of the hazard. Thus, a positive maximum eccentricity means a scan in the direction of the hazard. Note that, in some cases, if the maximum gaze scan and/or corresponding head scan happened to be on the opposite side of the hazard, then the eccentricity could be <0 degrees (i.e. negative). For participants with HFL, scans were categorized by whether the scan was toward the seeing or blind side.

Of the 680 events for those with HFL, 627 events remained after 30 events were not collected due to the experiment being stopped short from simulator sickness from 2 participants, and 23 events were not processed due to noise or technical issues with the data. For those with NV, we had 590 of 600 events with 10 events not being collected due to the experiment being stopped short from simulator sickness from 1 participant.

Statistical Methods

We evaluated the effect that HFL (blind side motorcycles in those with HFL, seeing side motorcycles in those with HFL, and seeing side motorcycles in those with NV) has on the detection variables (detection, safe detection, and early detection) using general linear mixed effect models (GLMs) constructed in MATLAB (fitglme.m: Mathworks, R2015a). Variance among participant, scenario, and event number were accounted for using a random effects structure that included random slopes and intercepts for all fixed effects to produce a maximal random effects structure.[30] For continuous variables (reaction time and car speed), we first checked visually their approximate normality and then utilized a linear mixed model (LMM) with the same procedure used for the Boolean detection variables. All of the maximal models converged.

Method of guidance (GPS or Lead Car) was not included as a factor in the models because preliminary analyses found no effect of guidance on any of our outcome measures, including detection, safe detections, early detections, gaze magnitude, and head magnitude (all P values > 0.37). Furthermore, there were no significant interactions between NV and HFL and guidance type (all P values > 0.15). A prior study with NV participants using exactly the same two guidance methods also found that guidance method had no effect on scans magnitudes.[21]

We evaluated whether there were differences in gaze and head scan magnitude between detected and not detection, safe and unsafe, and early and not early. We used Kruskal-Wallis tests given that the distributions of gaze and head scan eccentricities were not normally distributed.

Determining classification (i.e. prediction) of the detection variables (detection, safe detection, and early detection) using scanning (gaze and head eccentricity) was achieved using a repeated train and test approach.[31] For 5000 iterations, 75% of the data were randomly allocated to a training set and 25% to the testing set. For every iteration, we calculated for all criterions in the training set the Matthews Correlation Coefficient (MCC), which is a balanced metric that takes into account true and false positives and negatives and is appropriate for measuring binary classification performance for imbalanced datasets.[32,33] MCC is calculated using the following formula:

$$MCC = \frac{TP\,x\,TN - FP\,x\,FN}{\sqrt{(TP+FP)(TP+FN)(TN+FP)(TN+FN)}}$$

where TP corresponds to the number of true positives, TN corresponds to the numbers of true negatives, FP corresponds to the number of false positives, and FN corresponds to the number of false negatives for a given criterion. In other words, for each iteration and for a given threshold (e.g. 10 degrees), we calculated MCC from TP, TN, FP, and FN by comparing the true detection and not detection to the predicted detection and not detection. MCC ranges from -1 to 1, with zero representing random classification. We did not use accuracy because of the imbalance between detection and not detection. We selected the criterion that maximized MCC and then calculated MCC with that criterion in the testing set. Across the testing set iterations, if the 95% confidence interval (CI) of the classifications did not include 0 MCC, then we considered the classification significantly above or below chance. To determine whether one classifier performed better than another classifier, we conducted a two-sample Kolmogorov-Smirnov test on the distributions of testing set MCCs. If the classifier was significantly above chance, then we considered the final criterion to be the median of the criterions used in the testing set.

Results

Overall Detection Behaviors

Overall, those with HFL had fewer detections ($b = 3.6$, $se = 0.41$, $t = 9.0$, $P < 0.0001$), safe detections ($b = 1.3$, $se = 0.30$, $t = 4.4$, $P < 0.0001$), and early detections ($b = 3.1$, $se = 0.49$, $t = 6.3$, $P < 0.001$) than NV participants (Fig. 4). Those with HFL were also slower in their reaction time ($b = 0.73$, $se = 0.17$, $t = 4.4$,

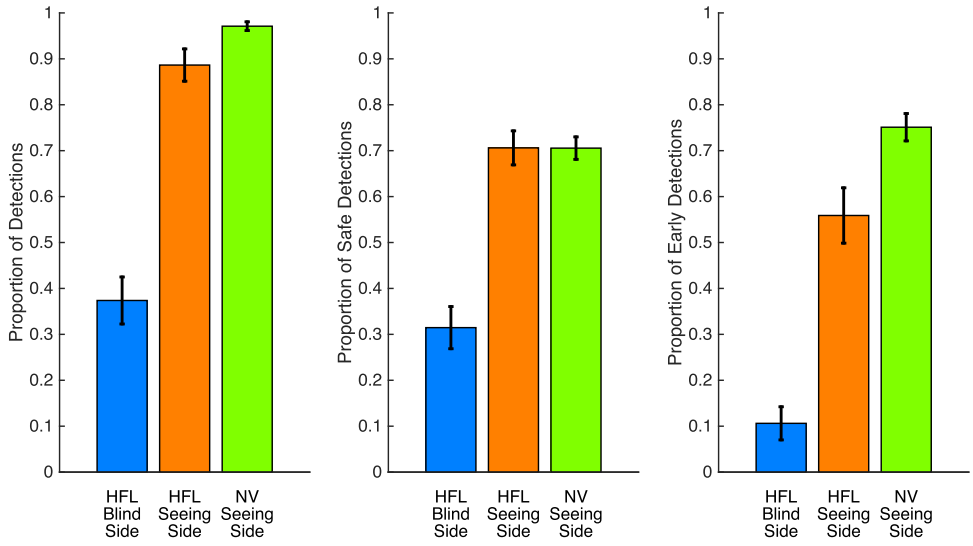

Figure 4. Average detection rates for those with HFL and NV. The proportion of detection (*left*), safe detections (*middle*), and early detections (*right*) are displayed for the motorcycles that appeared on the blind side and seeing side for those with HFL and seeing side for those with NV. Error bars are SEM.

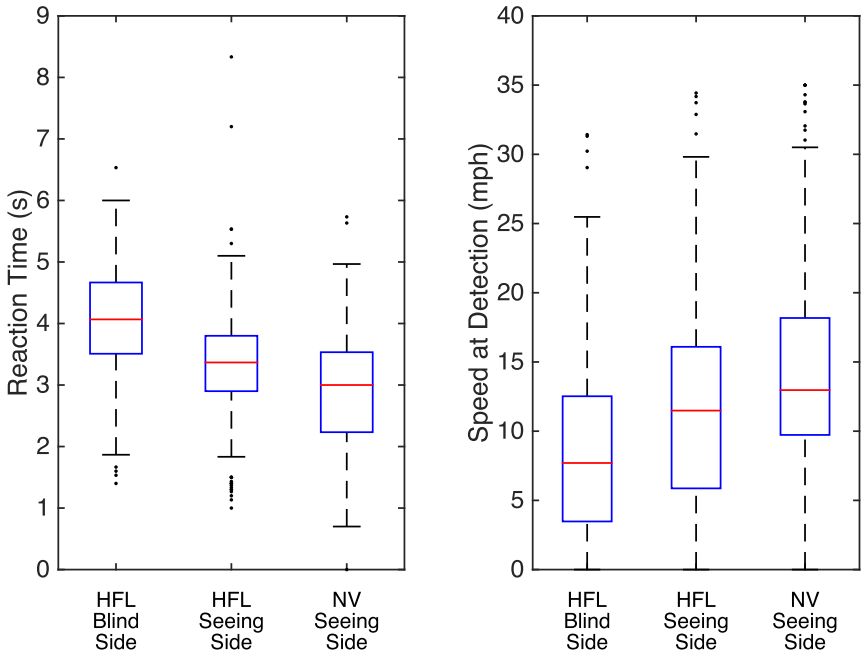

Figure 5. Boxplots summarizing reaction times (*left*) and speed at the time of the detection (i.e. horn press; *right*) are displayed for the motorcycles that appeared on the blind side and seeing side for those with HFL and seeing side for those with NV.

$P < 0.0001$) and in their driving speed at detection (b = 4.2, se = 1.4, t = 3.1, $P = 0.002$) than the NV participants (Fig. 5).

For those with HFL, there were fewer detections (b = 3.0, se = 0.38, t = 8.1, $P < 0.0001$), safe detections (b = 2.1, se = 0.29, t = 7.1, $P < 0.0001$), and early detections (b = 3.5, se = 0.41, t = 8.5, $P < 0.0001$) on the blind side than the seeing side (see Fig. 4). Further, those with HFL responded slower (b = 0.67, se = 0.1, t = 6.5, $P < 0.0001$) and were driving slower (b = 3.5, se = 1.1, t = 3.3, $P = 0.001$) when detecting motorcycle hazards on the blind side than seeing side (see Fig. 5).

Interestingly, when comparing detection performance for motorcycles that appeared on the seeing side, those with HFL had fewer detections (b = 1.6, se = 0.48, t = 3.4, $P = 0.001$) and early detections (b = 1.8, se = 0.5, t = 3.6, $P = 0.0004$) and slower reaction times (b = 0.6, se = 0.16, t = 3.6, $P = 0.0003$) than those with

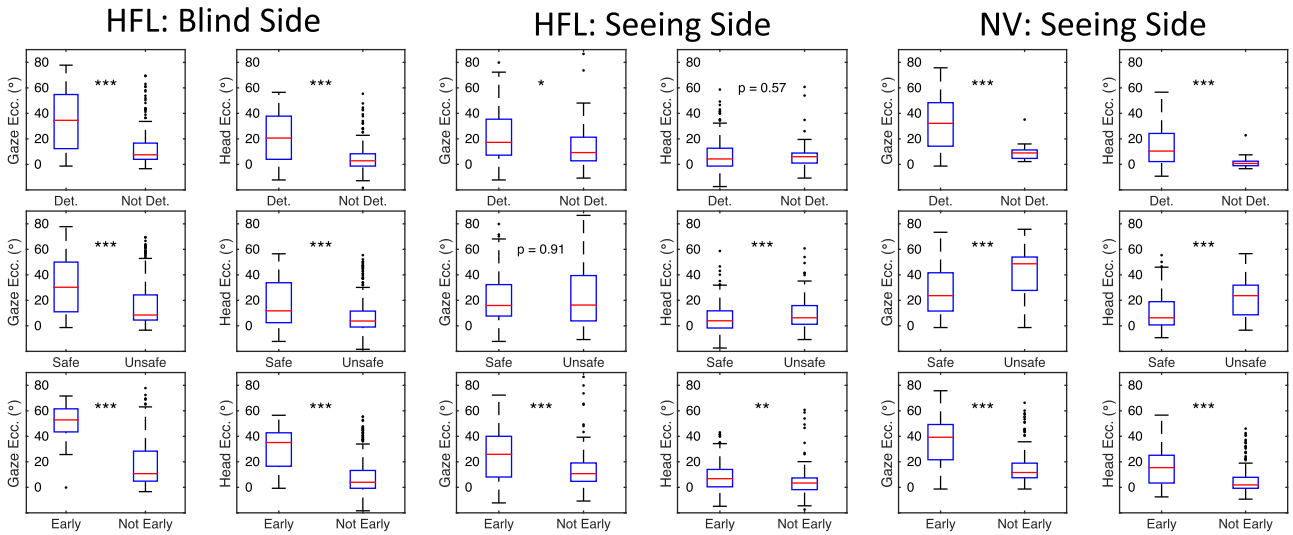

Figure 6. Box plots of maximum gaze and head eccentricity as a function of whether there was a detection (*top row*), safe detection (*middle row*), or early detection (*bottom row*). The *two leftmost columns* correspond to HFL blind side. The *two middle columns* correspond to the HFL seeing side. The *two rightmost columns* correspond to NV seeing side. Det. = detection. ***$P < 0.001$, **$P < 0.01$, *$P < 0.05$.

NV (see Fig. 4, Fig. 5). However, there was no significant difference in the proportion of safe detections (b = 0.14, se = 0.32, t = 0.4, $P = 0.67$), which is likely caused by those with HFL having a slower car velocity at the time of detection compared to those with NV (b = 3.3, se = 1.5, t = 2.2, $P = 0.03$).

Scanning and Detection Variables

The relationship between detection variables and scanning variables is shown in Figure 6. For blind side motorcycles in those with HFL, gaze scan (χ^2 [1] = 69.2, $P < 0.001$) and head scan (χ^2 [1] = 54.8, $P < 0.001$) magnitudes were significantly larger when the motorcycle was detected compared to when it was not detected. The same was true of gaze (χ^2 [1] =35.9, $P < 0.001$) and head scan (χ^2 [1] = 22.8, $P < 0.001$) magnitudes for safe detections and for gaze (χ^2 [1] = 53.7, $P < 0.001$) and head scan (χ^2 [1] = 39.6, $P < 0.001$) magnitudes for early detections.

On the seeing side, gaze scans (χ^2 [1] = 5.87, $P < 0.05$) were significantly larger in detections, but the same was not true of head scan magnitude (χ^2 [1] = 0.32, $P = 0.57$). Contrary to expectations, for safe detections, head scans were significantly larger for unsafe events compared to safe detections (χ^2 [1] = 6.7, $P < 0.001$). Gaze scan magnitude was not significantly different between safe and unsafe events (χ^2 [1] = 0.01, $P = 0.91$]. Gaze (χ^2 [1] = 29.3, $P < 0.001$) and head scan (χ^2 [1] = 10.7, $P < 0.01$) magnitudes were both significantly predictive for early detections on the seeing side in those with HFL.

For those with NV, gaze (χ^2 [1] = 20.3, $P < 0.001$) and head scan (χ^2 [1] = 13.6, $P < 0.001$) magnitudes were significantly larger in detections compared to failed detections. However, NV gaze (χ^2 [1] = 72.3, $P < 0.001$) and head scan (χ^2 [1] = 76.5, $P < 0.001$) magnitudes were significantly larger in unsafe events compared to safe detections (this counter intuitive finding is examined more in the "Scanning Criterion" section below). Last, gaze (χ^2 [1] = 110.2, $P < 0.00$) and head scan (χ^2 [1] = 63.9, $P < 0.001$) magnitudes were significantly larger in early detections compared to not early detections.

Predicting Detection Variables With Scanning Variables

For HFL participants, blind side motorcycle detection could be significantly predicted with gaze (95% CI = 0.24 to 0.59, $P < 0.001$) and head scan (95% CI = 0.24 to 0.59, $P < 0.001$) magnitudes (Fig. 7). Interestingly, head scan magnitude was a better predictor than gaze scan magnitude (K = 0.04, $P < 0.001$). Similar to detections, gaze (95% CI = 0.1 to 0.48, $P = 0.002$) and head scan (95% CI = 0.06 to 0.46, $P = 0.006$) magnitudes could significantly predict safe detections and gaze (95% CI = 0.20 to 0.63, $P < 0.001$) and head scan (95% CI = 0.11 to 0.61, $P < 0.005$) magnitudes could significantly predict early detections. For both safe (K = 0.16, $P < 0.001$) and early detections (K = 0.20, $P < 0.001$), gaze scan magnitude was a better predictor than head scan magnitude.

For those with HFL, seeing side detection could not be significantly predicted with gaze (95% CI = –0.20 to

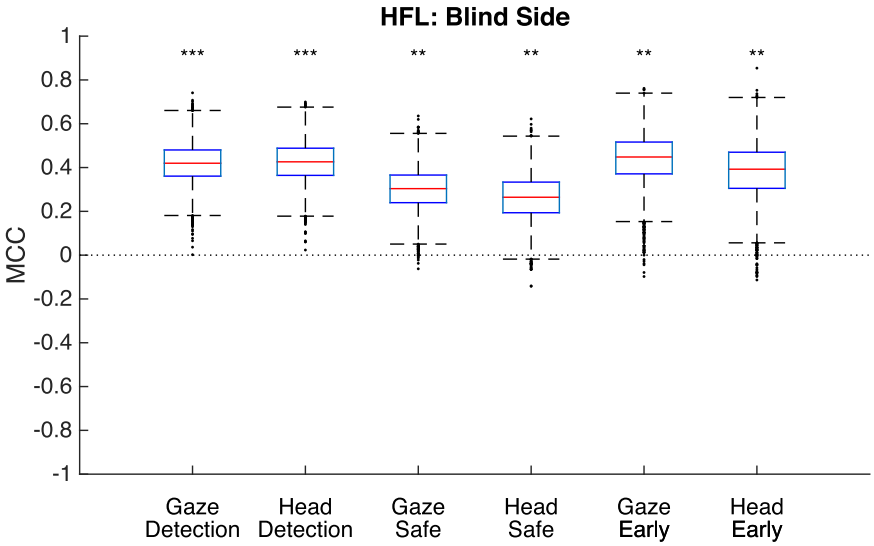

Figure 7. Boxplots summarizing prediction performance for the motorcycles that appeared on the blind side for those with HFL. The *dotted line* corresponds to chance prediction (i.e. random prediction) using Matthews correlation coefficient (MCC). ***$P < 0.001$, **$P < 0.01$, *$P < 0.05$.

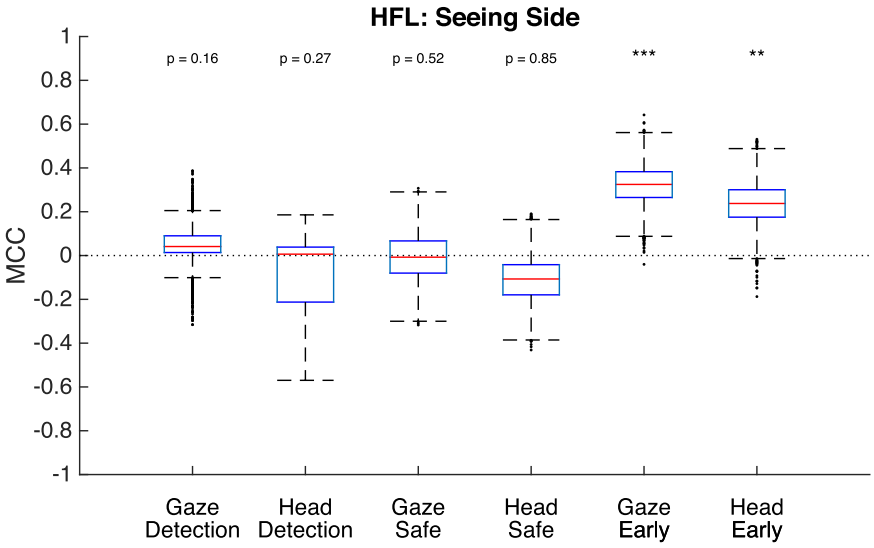

Figure 8. Boxplots summarizing prediction performance for the motorcycles that appeared on the seeing side for those with HFL. The *dotted line* corresponds to chance prediction (i.e. random prediction) using Matthews correlation coefficient (MCC). ***$P < 0.001$, **$P < 0.01$, *$P < 0.05$.

0.23, $P = 0.16$) or head scan (95% CI = –0.40 to 0.07, $P = 0.27$) magnitudes (Fig. 8). Similarly, gaze (95% CI = –0.22 to 0.18, $P = 0.52$) and head scan (95% CI = –0.30 to 0.10, $P = 0.85$) magnitudes could not significantly predict safe detections. Yet, seeing side early detections could be predicted with gaze (95% CI = 0.15 to 0.48, $P < 0.001$) and head scan (95% CI = 0.05 to 0.41, $P = 0.005$) magnitudes. Gaze scan magnitude was a better predictor than head scan magnitude for early detections (K = 0.38, $P < 0.001$).

For NV participants, gaze (95% CI = 0.02 to 0.33, $P = 0.02$) could significantly predict detection (Fig. 9), but head scan magnitude could not (95% CI = –0.06 to 0.27, $P = 0.047$). Interestingly, gaze (95% CI = –0.54 to –0.25, $P < 0.001$) and head scan (95% CI = –0.49 to –0.20, $P < 0.001$) magnitudes were significant predictors of safe detections, but in the opposite direction than we expected. That is, larger gaze and head scans could be used to predict unsafe events with gaze scan magnitude being a better predictor than head scan magnitude (K = 0.26, $P < 0.001$). Early detections

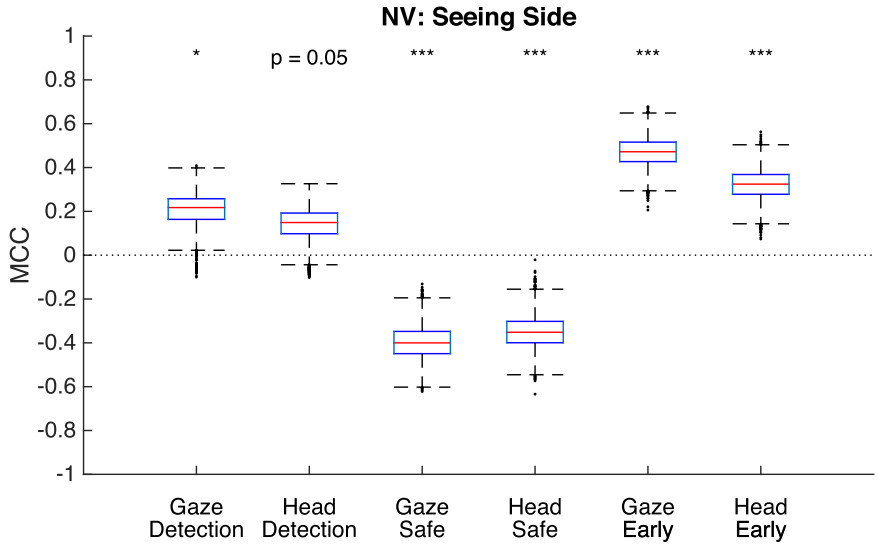

Figure 9. Boxplots summarizing prediction performance for the motorcycles that appeared on the seeing side for those with NV. The *dotted line* corresponds to chance prediction (i.e. random prediction) using Matthews correlation coefficient (MCC). ***$P < 0.001$, **$P < 0.01$, *$P < 0.05$.

Table 3. Criterions that Significantly Predicted Better Hazard Detection (More Detections, More Safe Detections, and More Early Detections)

	Scanning Criterions that Predicted Better Hazard Detection		
	Detection	Safe Detection	Early Detection
HFL: Blind side	Gaze: ≥ 22.8 degrees Head: ≥ 19.3 degrees	Gaze: ≥ 18.5 degrees Head: ≥ 19.3 degrees	Gaze: ≥ 33.8 degrees Head: ≥ 27 degrees
HFL: Seeing side			Gaze: ≥ 25.3 degrees Head: ≥ 9.0 degrees
NV: Seeing side	Gaze: ≥ 11.5 degrees	Gaze: ≤ 48.5 degrees[a] Head: ≤ 24.5 degrees[a]	Gaze: ≥ 20.5 degrees Head: ≥ 4.8 degrees

[a]For these two criterions, gaze or head scans less than the criterion resulted in more safe detections. All other criterions represent situations where gaze or head scans greater than the criterions resulted in more detections, unsafe detections, or early detections than gaze or head scans below the criterion.

could be significantly predicted with gaze (95% CI = 0.33 to 0.59, $P < 0.001$) and head scan (95% CI = 0.18 to 0.45, $P < 0.001$) magnitudes with gaze being a better predictor than head scan magnitude (K = 0.74, $P < 0.001$).

Scanning Criterion for Detection, Safe Detection, and Early Detection Classification

Next, we examined the criterions for the scanning variables that could significantly predict the detection variables (Table 3). For each criterion, magnitudes that exceeded these values meant successful detections unless otherwise stated. For motorcycles that appeared on the blind side of HFL participants, the gaze and head criterions for predicting detection were similar to the gaze and head scans that predicted safe detections. As expected, the gaze and head criterions for predicting early detections were larger than for detections. For seeing side events in those with HFL, only early detections could be significantly predicted with the maximum gaze and head scan magnitudes.

For those with NV, the gaze and head criterions for early detections were larger than the criterions for detection. Unlike all of the previous criterions though, magnitudes exceeding the gaze and head criterions for safe detections predicted unsafe events. That is, scanning below those criterions more often resulted in safe detections than scanning above those criterions. This is likely the result of unsafe detections occurring with higher driving speeds, which means that the

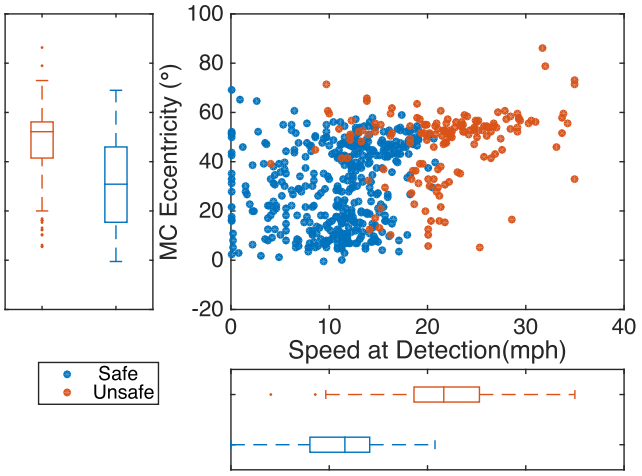

Figure 10. A scatterplot and boxplot showing the speed of the car at detection and the eccentricity of the motorcycle (MC) at the time of the end of the maximum gaze scan for safe (*blue*) and unsafe (*orange*) detections for NV participants.

individual is closer to the intersection and hence a larger gaze scan is needed for the motorcycle to be detected (Fig. 10).

Relationship Between Gaze and Head Scan Magnitudes

In many of the classifications, head scan magnitude was predictive of detection performance. Gaze and head maximum eccentricities were significantly correlated (Fig. 11, right column) for HFL blind side ($r = 0.86$, $P < 0.0001$) and seeing side ($r = 0.81$, $P < 0.0001$), and seeing side for those with NV ($r = 0.89$, $P < 0.0001$). As expected, gaze scans were significantly larger (see Fig. 11, left column) when the maximum head eccentricity was above than below the smallest of the significant head scan magnitude criteria (i.e. the smallest criterion out of detection, safe, and early; minimum χ^2 [1] = 157.6, $P < 0.0001$ between HFL blind, HFL seeing, and NV seeing with Kruskal-Wallis tests).

Discussion

Consistent with many prior studies,[6–11] we found that individuals with HFL detected fewer motorcycles on the blind than seeing side (37.4 vs. 88.6%) and had longer reaction times (4.1 seconds vs. 3.4 seconds). Furthermore, larger gaze and head scans were associated with detections on the blind side.[6,9,10] Individuals with HFL also had fewer detections on their seeing side than those with NV (88.6 vs. 97.0%), as found in other studies evaluating detection of pedestrians at large eccentricities at intersections.[6] These results highlight the importance of understanding the impacts of HFL on hazard detection performance[34] and the necessity of adequate compensatory strategies to see potential hazards approach from the side of their visual field loss.

Our main goal was to evaluate the minimum threshold (i.e. criterion) for gaze and head scan magnitudes that best predicted detection, given that making a large scan is a common technique included in rehabilitation programs aimed at improving compensation for visual field loss.[14,16] Importantly, we examined prediction of different types of detection (i.e. safe and early detections) of the peripheral motorcycle hazard because detections could occur early or late and could be safe or unsafe depending on the speed of the driver and distance to the intersection.

Blind side gaze and head scans could significantly predict whether a detection, safe detection, or early detection occurred, with criterions ranging from 18.5 degrees to 33.8 degrees and 19.3 degrees to 27 degrees for gaze and head respectively. The ability for blind side detections to be predictable was expected, given that individuals with HFL necessarily needed to scan in order to detect the motorcycle on their blind side. The criterions we found suggest that for those with HFL, the minimum head scan toward the blind side should be at least approximately 20 degrees when scanning on approach to an intersection. Importantly, this threshold encourages scans larger than individuals typically make with eye saccades (i.e. generally <15 degrees[20]), which is likely why head scan magnitude was also predictive of detection performance.

On the seeing side, gaze and head scans could significantly predict whether a safe or early detection occurred for those with NV. However, for those with HFL, only early detections could be significantly predicted (gaze = 25.3 degrees and head = 9 degrees), indicating that a large scan with a head movement component was needed for detection of the motorcycle before it reached the intersection (i.e. when at a large eccentricity) on the seeing side. Not being able to predict all detections on the seeing side in HFL participants could reflect a combination of two situations; (1) individuals could be relying on peripheral vision for detection on the seeing side (i.e. thus not making a gaze or head scan towards the hazard) and (2) individuals could scan past the motorcycle as it approaches (i.e. thus making a large gaze or head scan, but failing to detect the motorcycle). If the individual was not already attending to the motorcycle, then it may be missed because of the transient disruption of perception from the eye saccade[35,36] and because the motorcycle would now be in the blind portion of the visual field

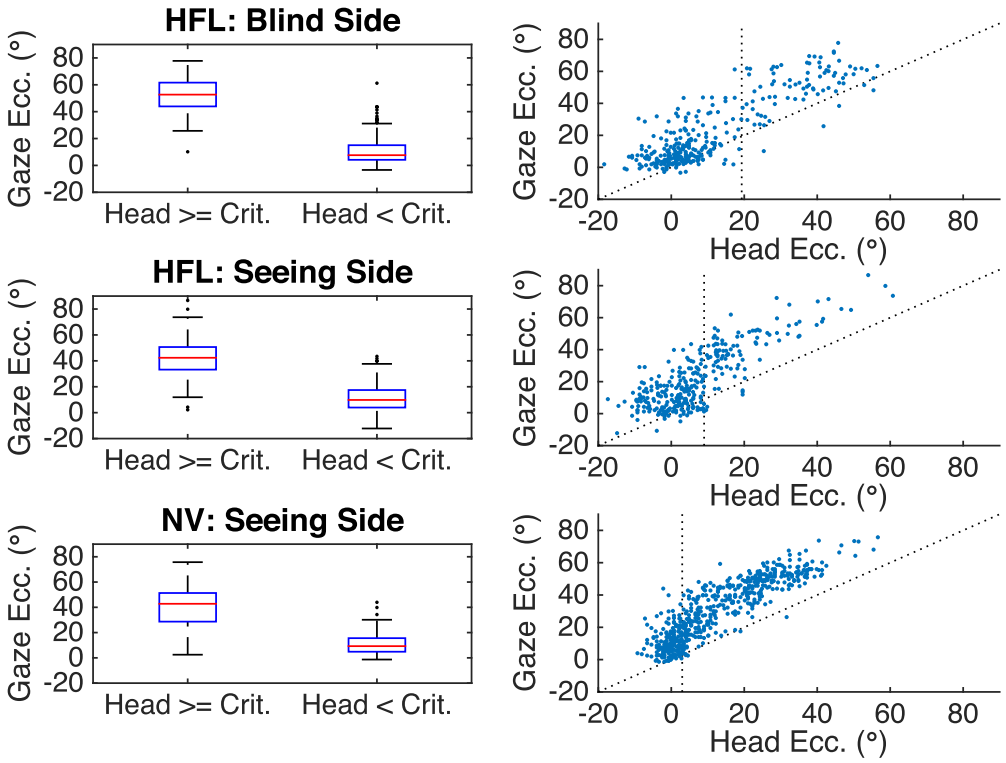

Figure 11. On the *left*, gaze eccentricity when head eccentricity exceeds the smallest (i.e. out of detection, safe, and early) significant head scan criterion between detection, safe detection, and early detection for HFL = blind side (19.3 degrees; *top left*), HFL = seeing side (9 degrees; *middle left*), and NV = seeing side (4.8 degrees; *bottom left*). On the *right*, scatter plots of head eccentricity and gaze eccentricity for the respective group. The *vertical dotted line* represents the criterion used in the box plots on the *left*. Crit. = criterion.

(i.e. scan across[37]). Nonetheless, finding a significant criterion for early detections on the seeing side in those with HFL indicates that scanning toward the seeing side is important for detecting hazards approaching from that side.

Interestingly, for those with NV, safe detections corresponded to smaller magnitude gaze and head scans than unsafe detections. Although this could indicate the cost of scanning too far, it is more likely a function of the increased driving speed associated with unsafe detections. Hazards approaching from the periphery at a constant speed were at greater eccentricities when participants drove more quickly than when they drove more slowly; hence larger scans needed to be made to detect hazards in unsafe situations associated with faster driving. Whereas this may have been true for all drivers, those with NV drove faster than those with HFL, which resulted in more instances of large scans during unsafe detections.

For each event, we analyzed only a single scan, the largest scan in the direction of the motorcycle. A similar approach was used by Bowers et al.[6,37] when evaluating the relationship between head scanning and detection of pedestrians at about 90 degrees eccentricity at intersections. Although analyzing the largest scan directly addressed our primary research question, it did not capture other aspects of scanning that might also be important for successful detection, such as the frequency of scanning or the role of eye-only scans. In contrast, other studies have considered all gaze scans (e.g. Refs. 8–11, 21). Using all of the gaze scans may be useful for understanding globally how individuals are scanning on approach to an intersection. However, here, we were interested in the scanning behavior that preceded detection (or lack of detection) and therefore could be used to better understand the relationship between scanning and detection of a hazard.

In analyzing the safety of detections, we took account of the speed of the vehicle as well as the distance to the intersection. This approach revealed an interesting finding with respect to seeing side detection performance. Specifically, whereas those with HFL detected fewer motorcycles on average than those with normal vision on the seeing side (88.6 vs. 97.0%), the rates of safe detections did not differ (70.6 vs. 70.6%)

because those with HFL drove more slowly. Driving slowly (provided it is not too slowly) may be another form of compensation that could improve detection performance in those with HFL when paired with more frequent and larger scans.

For both groups of participants, we found that when gaze scans predicted detection performance, head scans also generally predicted detection performance. This is likely because of the strong positive relationship between the gaze and head scan eccentricity. Further, gaze scans were typically larger than head scans, meaning that a large head scan was often paired with an even larger gaze scan. This finding has important implications for both training and the development of driver assistance devices. It may be easier for individuals to make larger gaze scans if they are encouraged to facilitate their gaze scan with a head scan, especially on approach to intersections. With regard to assistance devices, it is possible that the 20 degrees criterion could also be implemented in a device, which would monitor head position and alert individuals when they have failed to scan further than that criterion (Jing Xu, IOVS, 2019, 60, "ARVO E-Abstract," 1058). Tracking gaze in the real world is challenging because of the placement limitations of the equipment (i.e. so as to not obstruct the driver's view), wide ranging lighting conditions, and individuals requiring sunglasses or other eyeglasses to drive.[23] However, it is easier to track head position in real-world settings.[24,38] Thus, such a device that monitors and checks for large head scans may prove more feasible than one that relies on tracking gaze.

One limitation of the current study is that all of the motorcycle hazards started far in the periphery (at about 54 degrees eccentricity). Hazards can also start in more centrally located positions, such as an approaching car that takes a turn in front of the driver.[39] In hazards that appear from the straight-ahead position, it is likely that gaze and head scans will not be predictive. Further, peripheral hazards that approach at faster velocities or along different trajectories may require different magnitudes of peripheral scans to be detected. Future studies with varied hazard trajectories may be able to tease apart how different patterns of gaze movements relate to detection of different hazards.

Another potential limitation of this study is that many of the individuals with HFL had ceased driving since the onset of their visual field loss (because driving with HFL is not permitted in Massachusetts). However, the purposes of this study were not necessarily to understand how individuals with HFL compensate, but instead to evaluate scanning as a compensatory strategy from a rehabilitation perspective.

Overall, our results support the finding that making a large scan in advance of the intersection is beneficial for peripheral hazard detection by people with HFL. On the blind side, detection performance (i.e. detections, safe detections, and early detections) were all associated with larger scans and scan magnitude could be used to predict detection performance. On the seeing side, only early scans could be successfully predicted with gaze and head scan performance. These results present strong evidence that peripheral hazard detection is related to scan performance and suggest that individuals with HFL who scan beyond a criterion may be more likely to detect a hazard than not. The criterions we found could be utilized in rehabilitation or in the development of assistance devices to help individuals with HFL adequately compensate for peripheral hazard detection.

Acknowledgments

Supported in part by National Institutes of Health (NIH) Grant R01-EY025677, NIH Core Grant P30EY003790, and S10 – RR028122.

Funded in part by NIH Grants R01-EY025677, S10-RR028122, and P30-EY003790.

All authors contributed to the manuscript and conceived of the experiment. G.S. contributed to the programming, visualization, and analysis of the data.

Disclosure: **G. Swan**, None; **S.W. Savage**, None; **L. Zhang**, None; **A.R. Bowers**, None

References

1. Peli E. Low vision driving in the USA: who, where, when, and why. *CE Optometry*. 2002;5:54–58.
2. DVLA Drivers Medical Group. *For Medical Practitioners. At a Glance Guide to the Current Medical Standards of Fitness to Drive*. Swansea, UK: Driver Vehicle Licensing Authority; 2011.
3. European Parliament Council of the European Union. Commission Directive 2009/113/EC amending Directive 2006/126/EC of the European Parliament and of the Council on driving licenses. *Off J Europ Union*. 2009;L223:31–35.
4. Austroads . *Assessing fitness to drive for commercial and private vehicle drivers: Medical standards for licensing and clinical management guidelines*. Sydney, Australia: Austroads Ltd.; 2012.

5. Canadian Council of Motor Transport Administrators. Determining Driver Fitness in Canada: Part 1: Administration of Driver Fitness Programs and Part 2: CCMTA Medical Standards for Drivers. Edition 13. Available from: https://ccmta.ca/images/CCMTAMedicalStandardsDec12015finalcleancopyJune22016edit.bookmarkspdf.pdf. Accessed September 28, 2020.
6. Bowers AR, Ananyev E, Mandel J, Goldstein RB, Peli E. Driving with hemianopia IV: head scanning and detection at intersections in a simulator. *Invest Ophthalmol Vis Sci*. 2014;55:1540–1548.
7. Alberti CF, Goldstein RB, Peli E, Bowers AR. Driving with hemianopia V: do individuals with hemianopia spontaneously adapt their gaze scanning to differing hazard detection demands? *Transl Vis Sci Technol*. 2017;6:11.
8. Papageorgiou E, Hardiess G, Mallot HA, Schiefer U. Gaze patterns predicting successful collision avoidance in patients with homonymous visual field defects. *Vision Res*. 2012;65:25–37.
9. Bahnemann M, Hamel J, De Beukelaer S, et al. Compensatory eye and head movements of patients with homonymous hemianopia in the naturalistic setting of a driving simulation. *J Neurol*. 2015;262:316–325.
10. Kübler TC, Kasneci E, Rosenstiel W, et al. Driving with homonymous visual field defects: driving performance and compensatory gaze movements. *J Eye Mov Res*. 2015;8:1–11.
11. Hardiess G, Hansmann-Roth S, Mallot HA. Gaze movements and spatial working memory in collision avoidance: a traffic intersection task. *Front Behav Neurosci*. 2013;7:62.
12. de Haan GA, Melis-Dankers BJ, Brouwer WH, Tucha O, Heutink J. The effects of compensatory scanning training on mobility in patients with homonymous visual field defects: a randomized controlled trial. *PLoS One*. 2015;10:e0134459.
13. Tant ML, Brouwer WH, Cornelissen FW, Kooijman AC. Prediction and evaluation of driving and visuo-spatial performance in homonymous hemianopia after compensational training. *Vis Impair Res*. 2001;3:133–145.
14. Tant ML, Bouma JM, Kooijman A, Cornelissen F, Brouwer WH. Visual rehabilitation in homonymous hemianopia and related disorders. Brouwer WH, van Zomeren AH, Berg I, Bouma JM, Haan, eds. *Cognitive Rehabilitation: a clinical neuropsychological approach*. Amsterdam, UK: Boom; 2002.
15. Zihl J, Von Cramon D. Visual field recovery from scotoma in patients with postgeniculate damage: a review of 55 cases. *Brain*. 1985;108:335–365.
16. Zihl J. Eye movement patterns in hemianopic dyslexia. *Brain*. 1995;118:891–912.
17. Kerkhoff G, Münβinger U, Meier EK. Neurovisual rehabilitation in cerebral blindness. *Arch Neurol*. 1994;51:474–481.
18. Kerkhoff G, Münßinger U, Haaf E, Eberle-Strauss G, Stögerer E. Rehabilitation of homonymous scotomata in patients with postgeniculate damage of the visual system: saccadic compensation training. *Restor Neurol Neurosci*. 1992;4:245–254.
19. Guitton D, Volle M. Gaze control in humans: eye-head coordination during orienting movements to targets within and beyond the oculomotor range. *J Neurophysiol*. 1987;58:427–459.
20. Bahill AT, Adler D, Stark L. Most naturally occurring human saccades have magnitudes of 15 degrees or less. *Invest Ophthalmol Vis Sci*. 1975;14:468–469.
21. Savage SW, Zhang L, Swan G, Bowers AR. The effects of age on the contributions of head and eye movements to scanning behavior at intersections. *Transp Res Part F Traffic Psychol Behav*. 2020;73:128–142.
22. Swan G, Goldstein RB, Savage SW, Zhang L, Ahmadi A, Bowers AR. Automatic processing of gaze movements to quantify gaze scanning behaviors in a driving simulator. *Behav Res Methods*, https://doi.org/10.3758/s13428-020-01427-y.
23. Lee J, Muñoz M, Fridman L, Victor T, Reimer B, Mehler B. Investigating the correspondence between driver head position and glance location. *PeerJ Comput Sci*. 2018;4:e146.
24. Talamonti WJ, Kochhar DS, Tijerina L. Eye glance and head turn correspondence during secondary task performance in simulator driving. In Proceedings of the human factors and ergonomics society annual meeting. Los Angeles, CA: SAGE Publications; 2014;58(1):2224–2228.
25. Vanier M, Gauthier L, Lambert J, et al. Evaluation of left visuospatial neglect: norms and discrimination power of two tests. *Neuropsychology*. 1990;4:87.
26. Schenkenberg T, Bradford DC, Ajax ET. Line bisection and unilateral visual neglect in patients with neurologic impairment. *Neurology*. 1980;30:509–551.
27. Van Deusen J. Normative data for ninety-three elderly persons on the Schenkenberg line bisection test. *Phys Occup Ther Geriatr*. 1985;3:49–54.
28. Laureshyn A, Svensson Å, Hydén C. Evaluation of traffic safety, based on micro-level behavioural

data: Theoretical framework and first implementation. *Accid Anal Prev*. 2010;42:1637–1646.
29. Hupfer C. Deceleration to safety time (DST)-a useful figure to evaluate traffic safety. In ICTCT Conference Proceedings of Seminar 1997. Available at: https://www.ictct.net/conferences/10-lund-1997.
30. Barr DJ. Random effects structure for testing interactions in linear mixed-effects models. *Frontiers Psychol*. 2013;4:328.
31. Raschka S. Model evaluation, model selection, and algorithm selection in machine learning. arXiv.org. Available at: https://arXiv.org/abs/1811.12808.
32. Boughorbel S, Jarray F, El-Anbari M. Optimal classifier for imbalanced data using Matthews Correlation Coefficient metric. *PloS one*. 2017;12:e0177678.
33. Powers DM. Evaluation: from precision, recall and F-measure to ROC, informedness, markedness and correlation. *J Mach Learn Res*. 2011;2:37–63.
34. Bowers AR. Driving with homonymous visual field loss: a review of the literature. *Clin Exp Optom*. 2016;99:402–18.
35. Rensink RA, O'Regan JK, Clark JJ. To see or not to see: The need for attention to perceive changes in scenes. *Psychol Sci*. 1997;8:368–373.
36. Rensink RA. Seeing, sensing, and scrutinizing. *Vision Res*. 2000;40:1469–1487.
37. Bowers AR, Alberti CF, Hwang AD, Goldstein R, Peli E. Pilot study of gaze scanning and intersection detection failures of drivers with hemianopia. In: Proceedings of the Eighth International Driving Symposium on Human Factors in Driver Assessment, Training and Vehicle Design, June 22-25, 2015, Salt Lake City, Utah. Iowa City, IA: Public Policy Center, University of Iowa, 2015:240–246.
38. Smith RP, Shah M, da Vitoria Lobo N, inventors; University of Central Florida Research Foundation Inc UCFRF, assignee. Algorithm for monitoring head/eye motion for driver alertness with one camera. *United States Patent US*. 2005;6:927, 694.
39. Koustanaï A, Boloix E, Van Elslande P, Bastien C. Statistical analysis of "looked-but-failed-to-see" accidents: Highlighting the involvement of two distinct mechanisms. *Accid Anal Prev*. 2008;40:461–469.
40. Alberti CF, Peli E, Bowers AR. Driving with hemianopia: III. Detection of stationary and approaching pedestrians in a simulator. *Invest Ophthalmol Vis Sci*. 2014;55:368–374.
41. Bowers AR, Mandel AJ, Goldstein RB, Peli E. Driving with hemianopia. I: Detection performance in a driving simulator. *Invest Ophthalmol Vis Sci*. 2009;50:5137–5147.
42. Tant ML. Visual performance in homonymous hemianopia: assessment, training and driving. *Dissertation*. Groningen, The Netherlands: University Library Groningen; 2002.